

Chapter 5

Fabrication and characterization of porous silicon layers

In this chapter a complete description of the porous silicon fabrication system that we have established at the Department of Electronic, Electric and Automatic Engineering of the Universitat Rovira i Virgili is realized. In this description we also analyze the influence of the different elements used for the fabrication process on the characteristics of the fabricated porous silicon monolayers and multilayers, specially the differences between two types of electrochemical cells. Finally, the relations between the anodization parameters and the two most important physical characteristics of porous layers (refractive index and thickness) are presented. To conclude this chapter, the different methods used for the characterization of porous silicon layers are explained.

5.1. Fabrication System

In this section we describe in detail all the elements that are a part of the fabrication system. It is a self-controlled system created for the fabrication of porous silicon monolayers and multilayers that has been established at the Department of Electronic, Electric and Automatic Engineering at the University Rovira i Virgili. In this section, the importance of each element and its usefulness are explained, especially the electrochemical cell that is the most important part of all the process. The program realized for the control of the fabrication system is also explained.

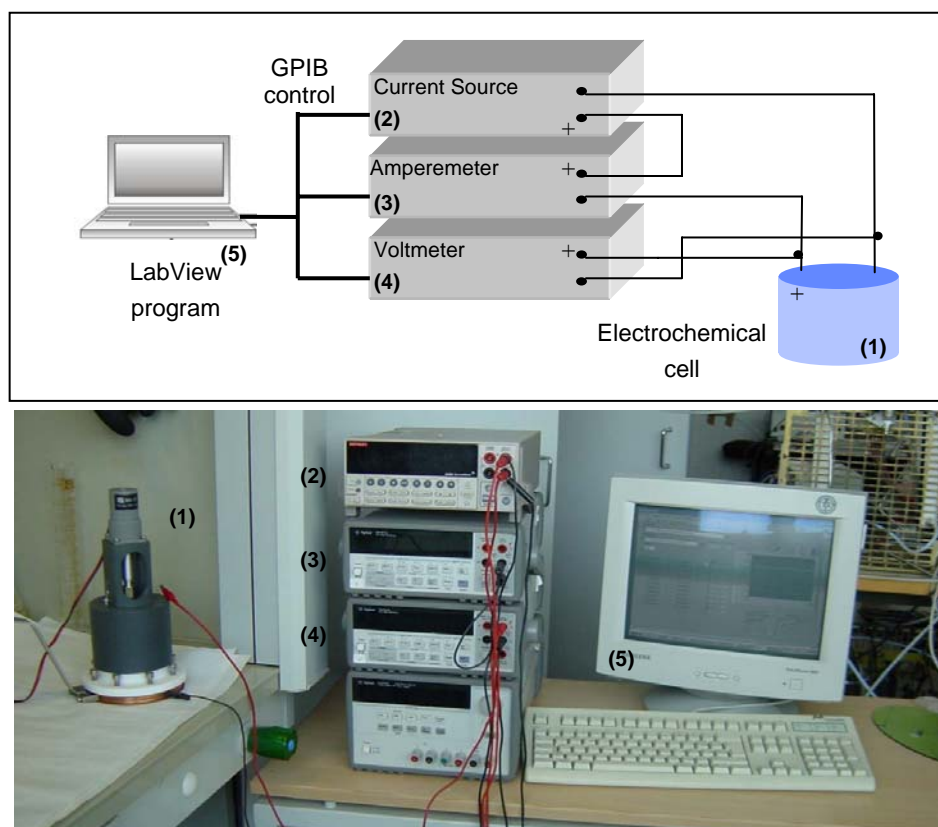


Fig. 5.1. a) Schematic of the designed porous silicon fabrication system b) Photograph of the system.

Fig. 5.1a shows the schematic of the fabrication system, wherea Fig. 5.1b shows its photograph. The main element of the system is the electrochemical cell (1), where the electrochemical etching of the silicon is realized. The current applied during the etch is provided by the current source (2). Two multimeters (3,4) are used for the measurement of the current and the voltage of the system during the etch process, respectively. They are used to supervise the etching process parameters. The whole system is controlled by a computer (5) where the developed LabView program controls continuously the two main parameters for the formation of the porous silicon structures: the current applied and the etching time.

In the next subsections, the elements of the system are described.

5.1.1. Electrochemical cell

The electrochemical cell is the most important part of the fabrication system because the homogeneity of the porous silicon samples depends on its structure. This conclusion has been obtained with the study of porous silicon monolayers and multilayers fabricated with two types of electrochemical cells.

5.1.1.1. Lateral-wafer electrochemical cell

The first type of cell that has been used for the fabrication process is the one that we have named lateral-wafer cell because its main characteristic is that the silicon wafer is located at the sidewall of the cell, as can be observed in the diagram of Fig. 5.2a. The **silicon wafer** acts as the anode and has a back-side contact that is a **metallic ring**. The front side of the wafer is sealed with an **O-ring**, so that only this part of the wafer surface is in contact with the electrolyte. The electrolyte is composed of high purity hydrofluoric acid (HF) in 40% aqueous solution diluted in ethanol (C_2H_5OH) at different concentrations. The **cathode** is made of platinum, a HF-resistant and conducting material. The **cell body** is a square-section teflon recipient. This material was selected because it

is a highly acid-resistant polymer. The stir of the electrolyte is realized with a **magnetic stirrer**. A photograph of this cell can be seen in Fig. 5.2b.

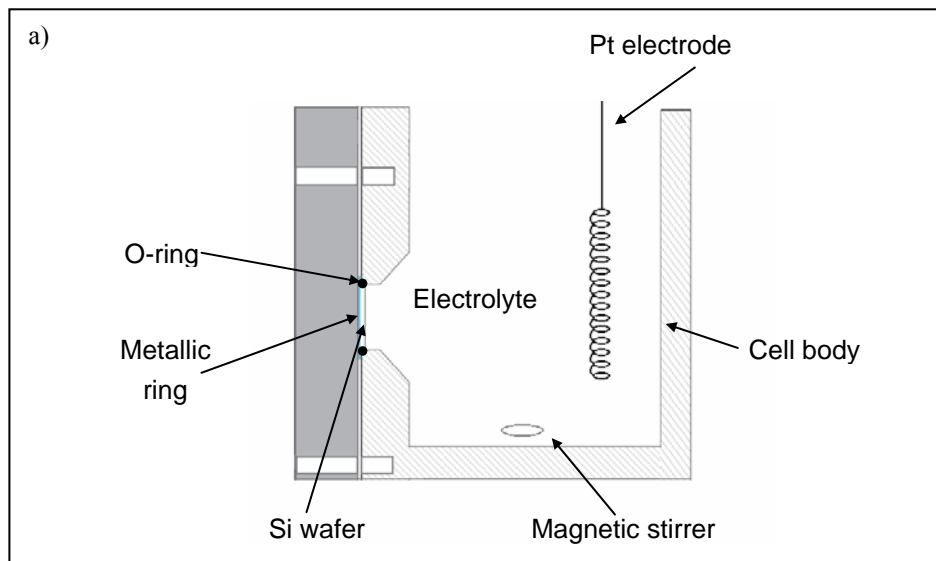


Fig. 5.2. The lateral-wafer cell used for the fabrication of porous silicon layers a) schematic of the cross sectional view. b) photograph of cell.

The main drawback of this cell is the inhomogeneity in porosity and thickness of the porous silicon layers. We have observed that the porous silicon

monolayers and multilayers fabricated with this lateral cell are highly inhomogeneous; in thickness, where the thickness from one point to another of the same sample can vary up to 30%, and in porosity where the refractive index may vary up to 0.5. This thickness variation can be observed in Fig. 5.3 where the cross section of a porous silicon monolayer fabricated with this cell has been observed with the Scanning Electron Microscope (SEM). The two different points of this section have different thickness and the difference between them is about 27 %. But it is not necessary to observe the samples with the SEM. At first sight it is possible to see the inhomogeneity of the fabricated monolayers in Fig. 5.4, where the color variation of the etched area indicates a variation of thickness and/or porosity.

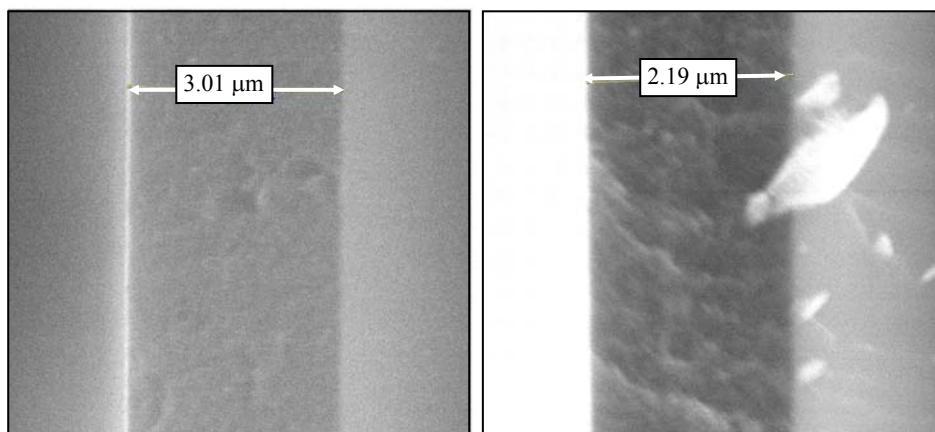


Fig. 5.3. SEM image of the cross section of a porous silicon monolayer fabricated with the lateral-wafer cell. The two images correspond to two different points of the same cross section. The thickness of the layer at each point is labeled.

The inhomogeneity of the porous silicon samples fabricated with this cell are most probably due to the bubbles that form and stick on the silicon surface. They must be removed and the concentration of HF has to be locally constant on the surface of the wafer. This type of cell does not facilitate the bubble

removal due in part to the lateral position of the sample, to the square section of the cell body, and to the limitations of the magnetic stirrer, that is low efficient for the large volume of the cell (around 800 ml).

To solve the inhomogeneity problems of the porous silicon samples due to the structure of the cell, a new electrochemical cell was designed and fabricated: the bottom-wafer cell.

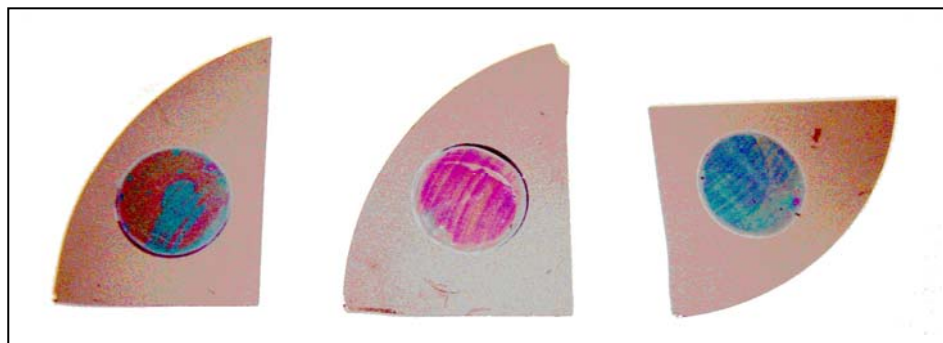


Fig. 5.4. Porous silicon layers fabricated with the lateral-wafer cell. The inhomogeneity of the etched area can be observed at first sight as the color varies indicating that either the porosity and/or the thickness of the layer changes.

5.1.1.2. Bottom-wafer electrochemical cell

The inhomogeneity problems of the former cell were mainly due to the lack of bubble removal on the surface of the wafer. This removal was hindered by the shape of the cell. To solve this problem, six structural variations have been introduced to the electrochemical cell design, as can be seen in Fig. 5.5a:

i) The cell body is a cylindrical-section recipient that facilitates the renovation of the electrolyte with the stirrer. Besides, the walls of the hole at the bottom of the recipient, realized for the contact of the electrolyte with the wafer, are not vertical but tilted to facilitate the renovation of the electrolyte and the removal of the bubbles on the surface of the wafer.

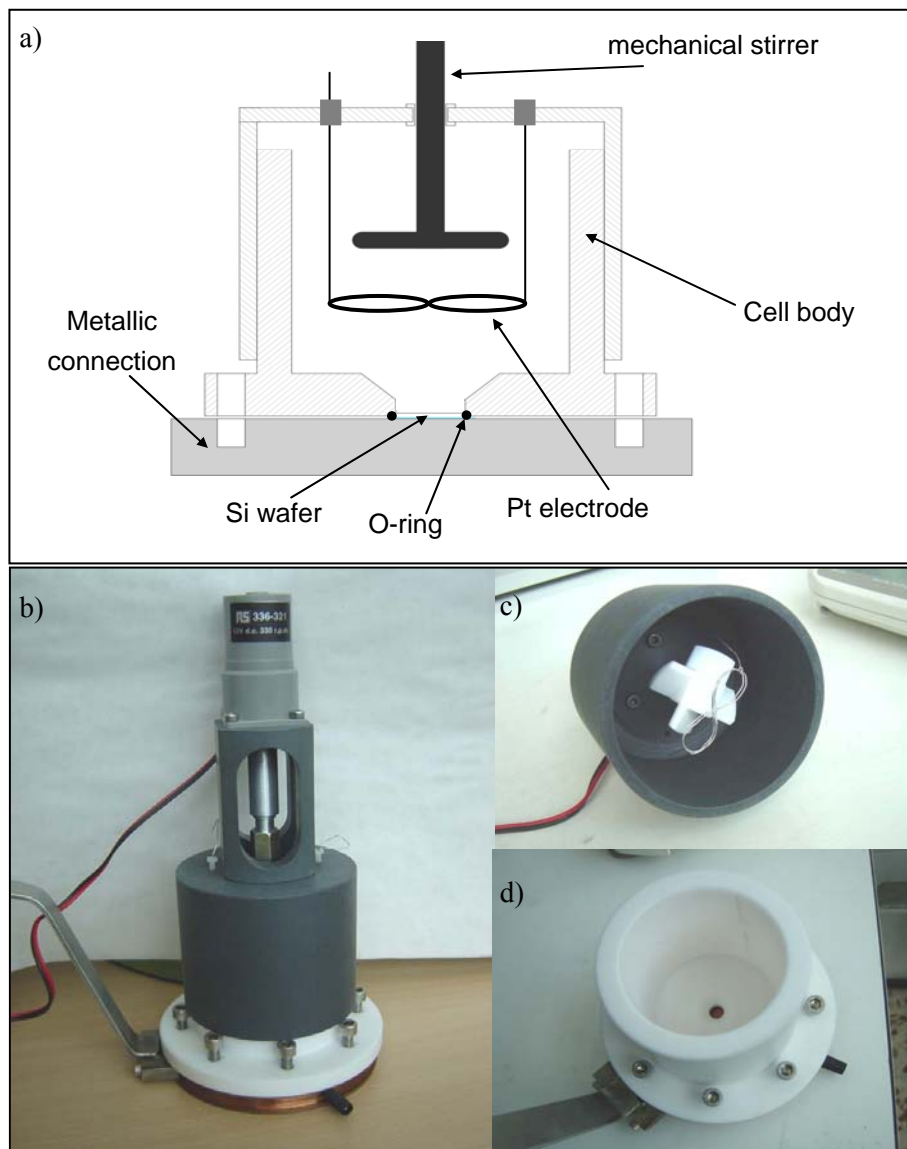


Fig. 5.5. Bottom-wafer cell designed and fabricated for the formation of porous silicon
a) schematic of the cross sectional view b) photograph of the fabricated cell, c) view of the stirrer and the Pt electrode, d) view of the inside part of the cell body.

ii) The stirrer here is mechanic and larger. Its shape has been specially selected to stir the electrolyte from bottom to top. The stirrer rotates because of a continuous motor. The rotation velocity is selected by adjusting the DC voltage applied to the motor.

iii) The wafer is situated at the bottom of the cell. With this variation, the bubbles formed on the surface are removed due to the stirrer effects and with the help of the gravity.

iv) The volume of the cell has been reduced. The dimensions of the cell are the smallest ones for the dimensions of the stirrer and the cathode. By this way, the quantity of electrolyte to stir is the lowest possible (around 200 ml in our case).

v) The back-side contact of the wafer is a copper disk instead of a ring. The disk enables a uniform contact on the whole area of the wafer. The copper disk has to be cleaned in order to remove the oxide film that is formed on it after many etching processes.

vi) The shape of the platinum cathode does not influence on the homogeneity of the samples, on the contrary, the distance between the wafer and the cathode does. If the distance is too short, the porous layers are inhomogeneous. It is from a certain distance when the samples are homogenous. It is preferable not to choose an excessively great distance since this implies that the height of the cell will increase, increasing therefore the amount of electrolyte to stir. In the case of our cell, about 4 cm is enough.

This new cell design enables the fabrication of homogeneous porous silicon monolayers and multilayers, as will be demonstrated with the characterization process realized with spectroscopic ellipsometry (see chapter 6). A photograph of the bottom-wafer cell can be observed in Fig. 5.5b.

The homogeneity of the porous silicon layers obtained with this electrochemical cell can be observed at first sight in Fig. 5.6a where it can be observed that the etched area of the layers presents a homogeneous color. The cross-section SEM image of one of the layers presented in Fig. 5.6a can be observed in Fig. 5.6b and Fig. 5.6c, where two different points of the same

section have been measured and the thickness is labeled. It can be observed that the thickness of the layer at the two different and separated points is the same.

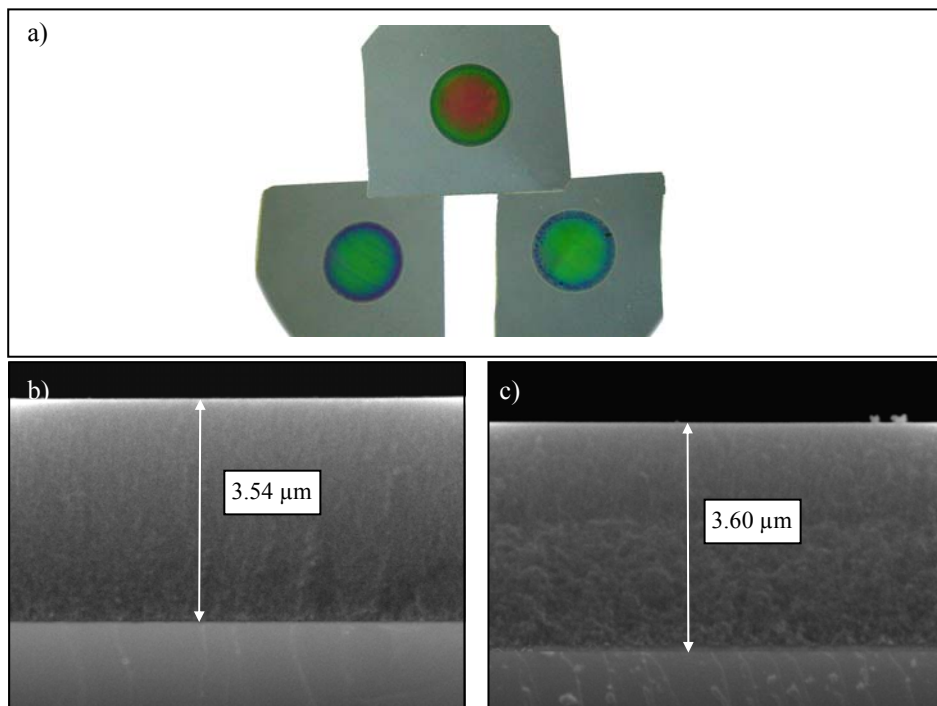


Fig. 5.6. a) Porous silicon layers fabricated with the bottom-wafer cell. The color of the etched area is very homogeneous at first sight indicating the homogeneity of the layer. b and c) SEM images of a porous silicon monolayer obtained with the bottom-wafer cell. Two different points of the same cross section are shown and their thickness is labeled.

5.1.2. Source for growth control

The process of pore growth can be realized either by controlling the anodic current or the potential. The most widely used method is the current control, because it allows a better control of the porosity, thickness and reproducibility of the porous silicon layer. For our fabrication system we have

realized current control using two different sources: a voltage source and a current source. The conclusions obtained with each of these two types of source are explained in the next subsections.

5.1.2.1. Voltage Source

The voltage source used for the system was an Agilent E3631A DC Power Supply. It was a part of the self-controlled system where two digital multimeters Agilent 34401A were used for the measurement and control of the voltage and current during the fabrication process. The measurements from the multimeters allowed the system to readjust the output of the voltage source continuously.

The only drawback of this system was the time that it needed to readjust the voltage source, the so-called response time of the system. This time was mainly due to the time needed by the multimeters to make a measurement and to communicate via GPIB with the computer. The response time of the system was about 400-500 ms and it affected the formation of the porous layers in two different ways:

- The transitions between two layers with different porosity were not rapid enough provoking an additional roughness between two porous layers with different porosity.
- The main problem appeared at the surface of the porous layer. The system required about 1 s during the beginning of the fabrication process to adjust the initial voltage. In microporous silicon growth, where the etching rate is very fast, this initialization time produced a residual porous layer, whose thickness and porosity depended on the initial conditions. In Fig. 5.7 the SEM image of a sample obtained with this system is shown, where the residual layer, created during the first seconds of the anodization process can be observed at the surface of the porous sample.

Although porosity was quite homogeneous within a layer and the response time was the only drawback of the voltage source system, this problem was important enough to lead us to use the current control.

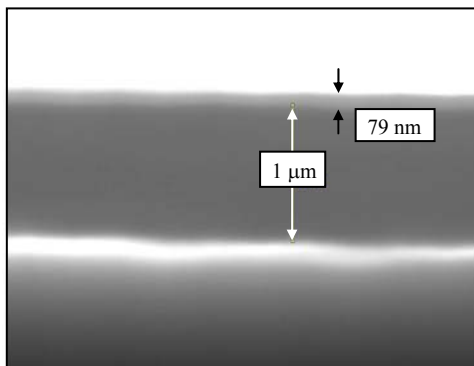


Fig. 5.7. SEM image of a monolayer obtained with the voltage source system. Its total thickness is 1 μm . We can also observe the residual layer created during the system adjust with a thickness 79 nm. The reflectivity spectrum of this sample measured with the FTIR also indicated that it is not a monolayer, but more that one layer was formed.

5.1.2.2. Current Source

The current source used for the fabrication system was a Keithley 2420 SourceMeter. This source enables a perfect control of the time and current applied during the growth and avoids the additional roughness between different porosity layers due to the response time of the system.

The homogeneity of a layer obtained with the current control can be observed in Fig. 5.8 where we can see that there is no residual layer at the upper part of the monolayer. For this reason, all the porous silicon layers presented in the next sections have been fabricated using this current source system.

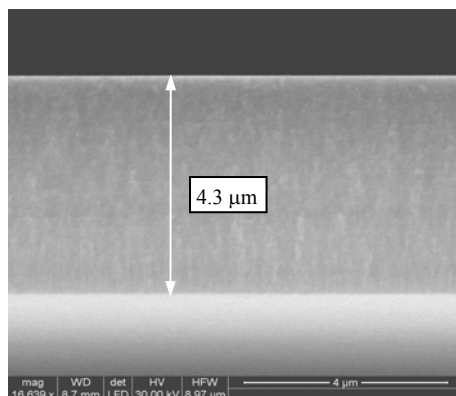


Fig. 5.8. SEM image of a porous silicon monolayer obtained using the current source. It is a homogeneous layer with thickness 4.3 μm .

5.1.3. Control Program

The fabrication process is completely controlled by a computer program. This program is a LabView virtual instrument realized to control the fabrication process of monolayers and multilayers of porous silicon with a very user-friendly interface. The program controls via GPIB the different elements of the system.

The main window of the program can be observed in Fig. 5.9. The user only has to introduce three data to the program:

- **Input File:** the path of the text file where the steps of current are defined, that is where the current profile is determined.
- **Output File:** the path of the text file where the program will write the measures realized during the fabrication process. This file is very useful for the user because it permits the comparison between the steps defined by the user and the steps applied by the system.
- **Delay:** the time between two consecutive measures.

The input file is a text file defined by the user with all the current steps and the duration time of each step. It is a very simple file where the first column is the duration time of the step and the second column is the current that must

be applied. Each row corresponds to a layer of the multilayer (or monolayer if only one step is defined).

The rest of elements of the program window indicate the data obtained during the fabrication process:

- **Graph**: Shows the current determined by the user and the current measured during the fabrication process in order to check if the process has been realized correctly.
- Arrays **Time** and **I measured**: The values plotted in the graph can also be read here numerically.
- **# Measured Points**: the number of measures that will be done during the formation process. It is calculated by the program from delay value introduced by the user.
- **Error**: Indicates if there has been any problem with the Source or the measurements during the fabrication process.

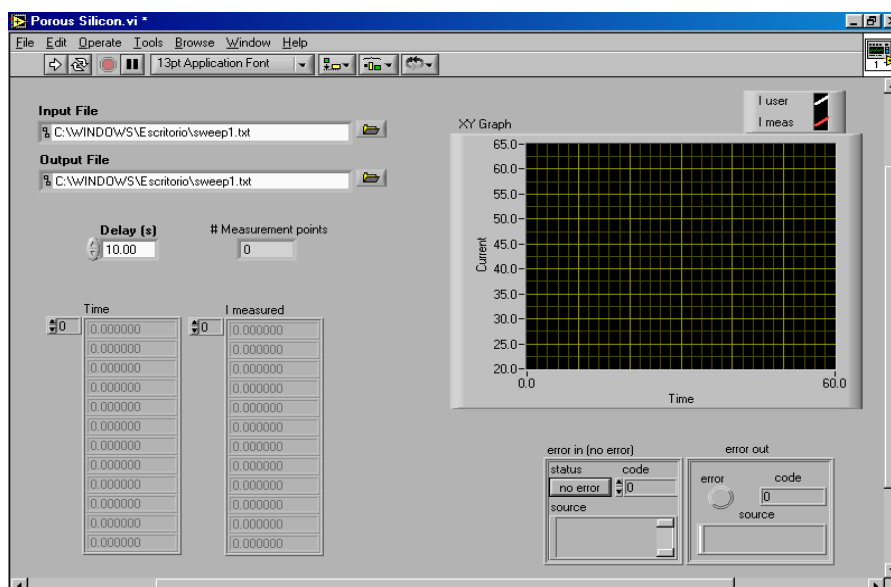


Fig. 5.9. Main window of the program that controls the fabrication process of porous silicon.

5.1.4. Electrolyte

The electrolyte used for the fabrication of porous silicon is an aqueous dilution of hydrofluoric acid (HF). The dilution is necessary due to the hydrophobic character of the clean silicon surface. In fact, ethanoic solutions infiltrate the pores, on the contrary pure aqueous HF solutions do not. This is very important for the lateral homogeneity and the uniformity of the porous silicon layer in depth. Moreover, the lateral homogeneity and the surface roughness can be reduced increasing the electrolyte viscosity [86].

The electrolyte that we have used for the fabrication of our porous silicon samples is composed of high purity hydrofluoric acid (HF) in 40% aqueous solution diluted in ethanol. We have used the electrolyte with approximately 15% concentration of HF. This concentration was chosen because many works have used it [48,176,135] and in [19] is considered to give a large porosity variation.

The importance of the use of ethanol for the dissolution has also been observed during the tests made for the starting of the fabrication process. It is well known that during the reaction there is a hydrogen release and bubbles are formed on the surface of the silicon wafer. In the beginning of the work, the aqueous HF was diluted in water instead of ethanol. The number of bubbles formed with this dissolution was so high that they produced high variations of voltage between anode and cathode, and resulting in a very inhomogeneous sample. The formation of bubbles during the growth was drastically reduced when ethanol was used for the dissolution instead of water. We have checked that with ethanol, the potential between anode and cathode does not vary during the growth of the porous layers.

5.1.5. Silicon wafers and sample preparation

During realization of this work, the wafers used for the formation of microporous silicon are p-type silicon wafers doped with boron. The use of p-type wafers instead of n-type wafer permits us not to use back-side illumination for the generation of minority carriers (see chapter 2).

The resistivity of the wafer influences on the hardness/toughness of the microporous structure. At the beginning of this work, the growth of porous silicon was realized with three different resistivity wafers: 5-7 Ω , 1-10 Ω , and 10-20 m Ω . The two former ones are considered high resistivity wafers whereas the latter is a low resistivity wafer.

The porous silicon layers obtained with the high resistivity wafers (low doped) were very fragile, the surface of the wafer was very rough and some parts of the etched zone detached from the wafer either during the fabrication process or during the drying process. These results were obtained even for very low current densities (5 or 10 mA/cm²). One of these porous wafers obtained with low doping substrates can be observed in Fig. 5.10a.

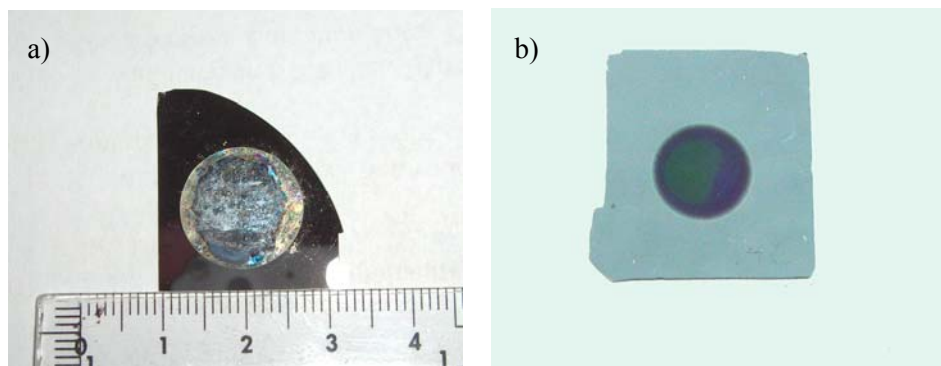


Fig. 5.10. Photograph of two porous silicon layers obtained with (a) a low doping silicon (b) a high doping silicon wafer.

On the contrary, the porous silicon layers obtained with low-resistivity wafers (high-doped) are strong and robust and their surface is flat, as can be seen in Fig. 5.10b. Furthermore, the very low resistivity of these wafers enables a good contact between the wafer and its back-side metallic connection (copper disk), without the need of a high dose implantation on the back surface of the

wafer. For these reasons, this type of wafers has been used for the fabrication of the porous silicon layers presented in this work.

The preparation of the silicon wafer for the porous silicon fabrication is very simple. Microporous silicon consists of the growth of disordered pores in the silicon wafer, therefore no lithography or preparation of the wafer is required. The preparation of the silicon wafer before the etching process is reduced to the removal of the oxidation of the wafer surface due to ambient conditions. This oxidation is easy to eliminate by immersing the wafer in low concentration (5 %) HF solution for a few minutes.

Drying of the porous silicon samples

Once the porous silicon has been formed, the etched wafer has to be dried. Due to large capillary stress, drying of samples is a critical step and can result in extended cracking if special procedures are not followed. Methods to reduce or eliminate the capillary stress include pentane drying, supercritical drying, freeze drying and slow evaporation rates.

Pentane drying is the easiest to implement. Pentane has a very low surface tension, and shows no chemical interaction with porous silicon (unlike ethanol). Using pentane as drying liquid enables to reduce strongly the capillary tension, but since water and pentane are non-miscible liquids, ethanol or methanol have to be used as intermediate liquids. Using this drying technique porous silicon layers with high porosity exhibit no cracking pattern after drying. All the porous silicon samples realized during this work have been dried with pentane.

5.1.6. Fabrication of porous silicon monolayers and multilayers

As all the elements of the fabrication system and their utility have been explained in the previous subsections, we can summarize the fabrication process of porous silicon monolayers talking about these elements. In the electrochemical cell, the surface of a silicon wafer, contacted on the back, is in contact with the electrolyte. After applying a current, controlled by the current source, between the wafer backside contact and the electrode in the electrolyte, a pore growth by silicon dissolution starts. The figure with the whole system has been presented in Fig. 5.1. The current density determines the porosity of the porous silicon layer and the time that it is applied determines the thickness of the layer.

The formation of multilayer structures of porous silicon opens a broad range of applications, some of them simulated and designed in chapters 3 and 4. The main advantage of porous silicon multilayers is the almost free combination of layers with different porosity and thickness because these two parameters can be easily determined during the formation process of porous silicon.

There are two main ways of producing porous silicon multilayers [177,92]: by periodically varying the etching parameters, such as for example the current density; or by using periodically doped substrates and maintaining constant the various etching parameters. All the multilayers fabricated during this work have been obtained with the first method, that is varying the etching parameters and using homogeneously doped substrates. This method is used by almost all the other authors that fabricate porous silicon multilayers [39,81,178,179].

This method is based onto the following statements:

- the etching process is self-limited (once a porous layer is formed, the electrochemical etching of this layer stops).
- the etching occurs mainly in correspondence of the pore tips.
- the porosity depends only on the current density once the other etching parameters are kept fixed.

The application of a current density during a certain time results in the formation of one layer. A change of the current density yields the variation of porosity and as a result another layer with different refractive index is formed during the application of this second current density. In Fig. 5.11 we can observe the schematic of the growth of a porous silicon multilayer.

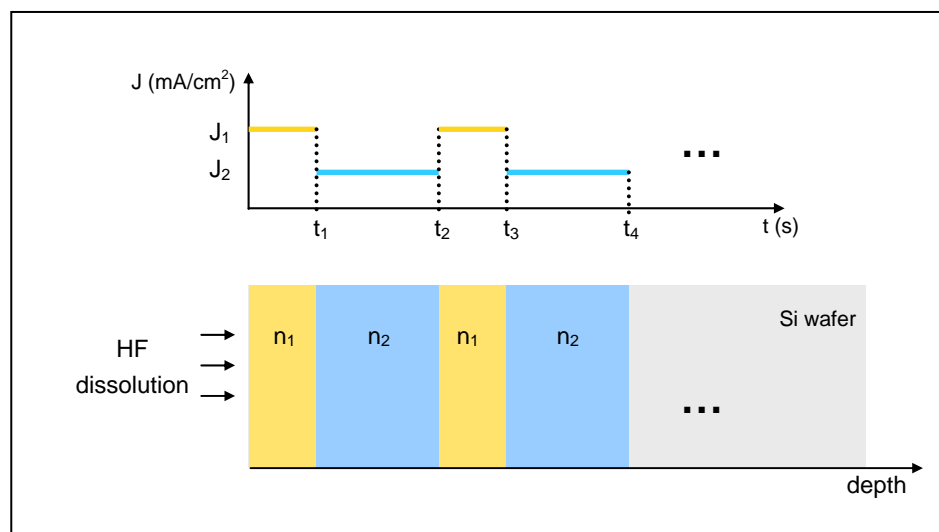


Fig. 5.11. Schematic of the formation process of a porous silicon multilayer (top) the time dependence of the current density (bottom) the formed porous silicon layer for each current density.

Hence, we can conclude that the variation of the current density during the etch process leads to the variation of the refractive index (porosity) in the etching direction only at the etch front. We can say that the current-versus-time profile is transferred to the porosity-versus-depth profile, that is refractive index-versus-depth profile.

This procedure has been used for the formation of all the multilayers fabricated during this thesis. Fig. 5.12 shows the SEM image of a multilayer formed by the periodic repetition of two layers with different refractive index.

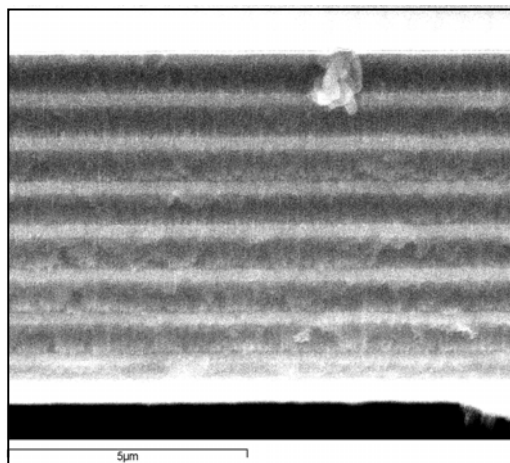


Fig. 5.12. SEM image of one of the fabricated porous silicon multilayers consisting of two layers with different refractive index repeated periodically.

5.2. Characterization of porous silicon layers

Once implemented the fabrication system, several porous silicon layers (monolayers and multilayers) have been fabricated. These layers have been measured with different techniques: Scanning electron microscopy, Fourier Transform Infrared Spectroscopy and Spectroscopic Ellipsometry. By processing these measurements, we can obtain different characteristics like the refractive index, thickness, anisotropy, etc.

This section is divided in two different parts. The first part is devoted to a brief explanation of the different techniques used for the measurement of the porous layers. The second part explains the two methods used for processing these measurements for determining the two main features of porous silicon layers: refractive index and thickness.

5.2.1. Measurement techniques

5.2.1.1. Scanning Electron Microscopy

The Scanning Electron Microscope (SEM) is a microscope that uses electrons rather than light to form an image. Some advantages of the SEM are the large depth of field, which allows a large amount of the sample to be in focus at a given time. The SEM also produces images of high resolution, which means that closely spaced features can be examined at a high magnification. Preparation of the samples is relatively easy since, most SEMs only require the sample to be conductive. The combination of higher magnification, larger depth of focus, greater resolution, and ease of sample observation makes the SEM one of the most widely used instruments in research areas today.

The SEM is an appropriate method to observe porous silicon layers. It is very useful for the determination of the structure, size and shape of the pores [41], especially for meso and macroporous silicon. For microporous silicon, the SEM image of the cross section of a porous silicon layer shows the porous zone clearly distinguished from the substrate [44,176]. For this reason it has been used for the thickness estimation of our monolayers.

SEM images present different gray levels depending on the porosity of the layers [39,180]. For this reason, the thickness of the different layers of a multilayer can be measured. It has also been used for evaluating the homogeneity of the porous silicon layers, for analyzing the interfaces, for observing the roughness between different porous layers and for the calculation of the etching rate [79,115,92,181]. Fig. 5.13 shows the SEM image of a porous silicon multilayer where the different layers can be clearly seen.

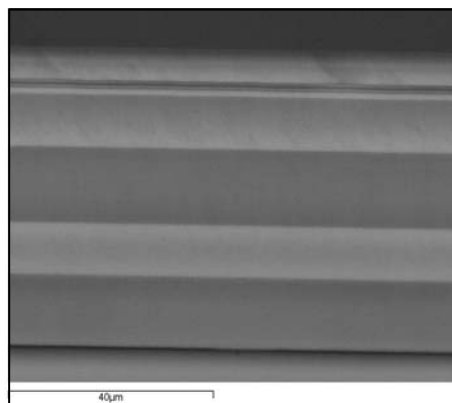


Fig. 5.13. SEM image of a porous silicon multilayer. It consists of two layers with different refractive index repeated two times.

5.2.1.2. Fourier Transform Infrared Spectroscopy

A Fourier Transform Infrared (FTIR) Spectrometer is a spectral instrument that collects and digitizes the interferogram, performs the FT function and displays the spectrum. Basically, the FTIR illuminates the sample and calculates the reflected, transmitted or absorbed light for a wavelength range [80]. It is used for the optical characterization of layers [39,80,98182-184].

The FTIR spectrometer used for the measurement of our porous silicon samples is a Bruker Vertex 70. The photograph of the spectrometer can be observed in Fig. 5.14. The spectra obtained with the FTIR, that have been used for the analysis of the porous layers, are the reflectivity and the transmission spectra for the wavelength range from 1 to 4 μm .



Fig. 5.14. Photograph of the FTIR spectrometer Bruker Vertex 70 used for the measurement of the porous silicon layers. The setup for the measurement of the reflectivity spectrum is placed.

5.2.1.3. Spectroscopic Ellipsometry

Spectroscopic Ellipsometry is a non-destructive optical technique widely used that measures the polarization of the light reflected on the surface of a sample in a wavelength range [185]. The ellipsometric measurements are evaluated to obtain the complex refractive index (n and extinction coefficient k), the interface roughness, the thickness and the composition of films [186]. One of the most widely used evaluation methods is the Bruggemann Effective Medium Approximation (EMA) [187-190].

For porous silicon layers, we have used ellipsometry to determine the optical properties of the layers and the substrate [79,187,191,192]. The thickness and refractive index of monolayers and multilayers have been calculated and the porosity of the layers, very difficult to determine with the other methods, has been estimated. Besides, the anisotropy of porous silicon layers with different porosity has been analyzed.

The complete analysis and characterization of the porous silicon layers realized with ellipsometry is extensively explained in chapter 6.

5.2.1.4. Atomic Force Microscopy

Another technique widely used for the analysis of porous silicon layers is the Atom Force Microscopy (AFM). AFM images are obtained by measurement of the force on a sharp tip (insulating or not) created by the proximity to the surface of the sample. This force is kept small and at constant level with a feedback mechanism. When the tip is moved sideways it will follow the surface contours [193]. By this way, three dimensional images of the surface of the samples are obtained.

The AFM studies are focused on the characterization, at nanometric scale, of the porous silicon layers, specially used for the study of layer inhomogeneities [194], surface roughness of the substrate [195], and morphology of porous silicon [196-199]. For many studies, AFM is applied together with another optical characterization or morphological technique. [200-203].

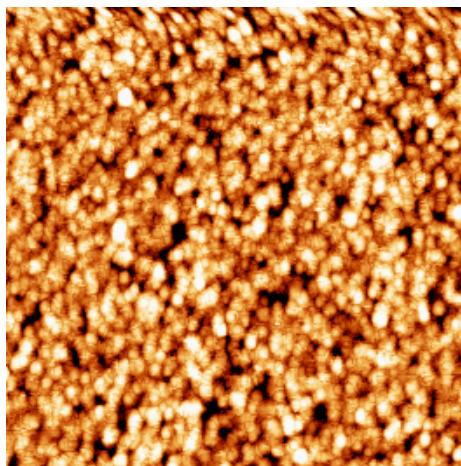


Fig. 5.15. AFM image of the surface of a porous silicon monolayer.

For our porous silicon layers, the AFM has been used for the study of the surface of the porous layers. Fig. 5.15 shows the AFM image of a porous silicon layer. These layers will be used in the near future as templates for the fabrication of liquid crystal photonic crystals where the knowledge of the surface contour of the layer is very important.

5.2.2. Mathematical methods for the determination of the refractive index and thickness

Each of the two mathematical methods explained here for the calculation of the refractive index and thickness use some of the measurements explained in the previous section. For the comparison of both methods, these characteristics are calculated for an example porous silicon monolayer and, at the end of this section, these results are evaluated.

5.2.2.1. Measurement of interference fringes

A very simple method for evaluating the refractive index of a film material is to measure the interference fringes, resulting from multiple reflections, to obtain the optical thickness. This method has been used by different authors only for normal incidence [19,103]. Here we develop the expressions for the refractive index calculation for any incidence angle.

Fig. 5.16 shows a typical arrangement for thin-film interference. Light traveling from one medium with refractive index n_0 encounters a thin film with refractive index n . Some of the light is transmitted through the film and some other is reflected. Thin film interference involves interference between light reflecting from the top surface of the film and light reflecting from the bottom surface of the film. For the case of porous silicon layers, the incident medium is air, being its refractive index $n_0=1$.

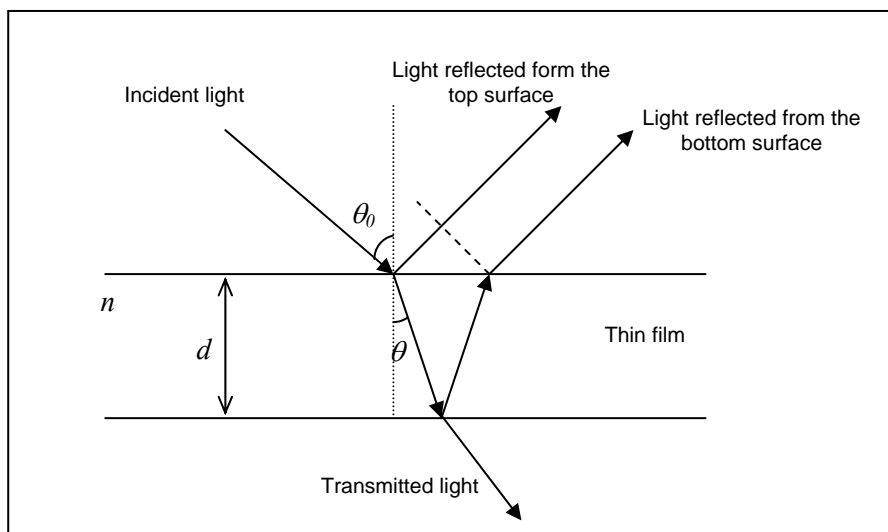


Fig. 5.16. Schematic of the light beam reflection when it arrives to a thin film with thickness d and refractive index n with an incident angle θ_0 .

The reflectivity spectrum of the film is characterized by the multiple interference fringes caused by the air-porous silicon and porous silicon-silicon interfaces. By assuming that the porous silicon film has parallel surfaces and that the refractive index is a smooth function of the wavelength, it is possible to deduce from the wavelength position of adjacent reflectance maxima the value of the refractive index [204]. The condition for a constructive interference is:

$$2nd \cos\theta = m \lambda_m \quad \text{for } m=0,1,2, \dots \quad (5.1)$$

Therefore the expressions for two consecutive maxima are:

$$m = \frac{2nd \cos\theta}{\lambda_m} \quad \text{and} \quad m+1 = \frac{2nd \cos\theta}{\lambda_{m+1}} \quad (5.2)$$

From these two expressions we obtain:

$$2nd \cos \theta \left(\frac{1}{\lambda_{m+1}} - \frac{1}{\lambda_m} \right) = 1 \quad (5.3)$$

Instead of θ we express Eq. (5.4) in terms of the incidence angle θ_0 , applying Snell's law:

$$n \sqrt{1 - \sin^2 \theta} = n \sqrt{1 - \frac{\sin^2 \theta_0}{n^2}} = \left[2d \left(\frac{1}{\lambda_{m+1}} - \frac{1}{\lambda_m} \right) \right]^{-1} \quad (5.4)$$

The resulting expression of the refractive index n for any incidence angle θ_0 is:

$$n = \sqrt{\sin^2 \theta_0 + \left[2d \left(\frac{1}{\lambda_m} - \frac{1}{\lambda_{m+1}} \right) \right]^{-2}} \quad (5.5)$$

where θ_0 is the incidence angle, λ_m is the wavelength of the m^{th} maximum of the reflectivity spectrum and d is the thickness of the monolayer.

Equation (5.5) has been used for the calculation of the refractive index of all the monolayers fabricated during this work. To apply this equation, two different measurements were realized to the monolayers. First, the reflectivity spectrum was measured for different angles of incidence with the Fourier Transform Infrared (FTIR) Spectrometer Bruker Vertex 70. By this way, the wavelengths corresponding to maximum reflectivity were determined. Fig. 5.17a shows the reflectivity spectrum of a monolayer fabricated by applying $J=20 \text{ mA/cm}^2$ for 120 s. It was measured for incidence angle $\theta_0=12^\circ$ and the different interference fringes can be observed.

The second value required for the application of Eq. (5.5) is the thickness of the monolayer, measured with SEM. In Fig. 5.17b the SEM image of the monolayer with the reflectivity spectrum shown in Fig. 5.17a can be observed.

The refractive index of this monolayer has been calculated using Eq. (5.5). It varies from 1.97 to 1.83 for the wavelength range between 1 μm and 4 μm , which demonstrates that the refractive index of porous silicon within this wavelength range is not constant (for more details see section 5.3.1).

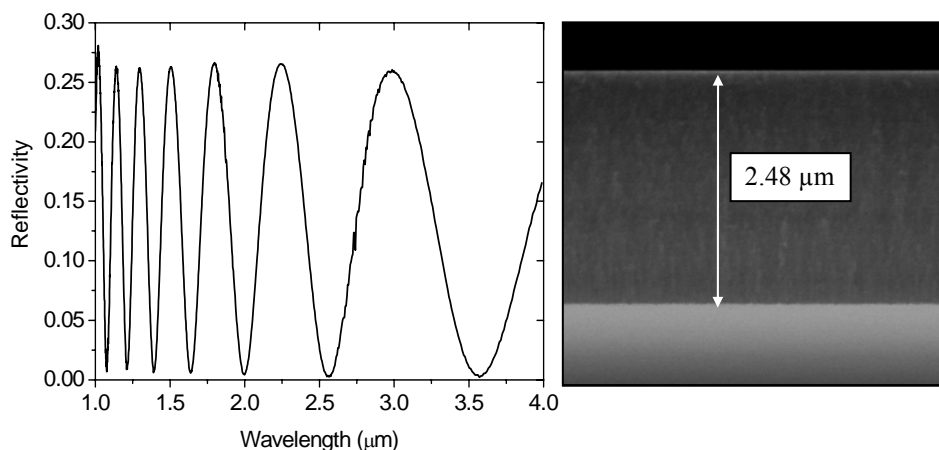


Fig. 5.17. (a) Reflectivity spectrum of a porous silicon monolayer obtained with $J=20$ mA/cm^2 and $t=120$ s, for $\theta_\theta=12^\circ$ (b) SEM image of the cross section of the same porous silicon monolayer. Its thickness is 2.48 μm .

The main advantage of this method is that it is fast and easy. The main disadvantage is that the estimation of thickness with SEM is not very accurate, which can introduce an error of about 5% on the refractive index.

5.2.2.2. Spectrum analysis fitting

This is a procedure for the optical characterization of thin-film monolayers and stacks from spectrophotometric and/or ellipsometric data. It consists of a least-squares fitting of the simulated spectrum to a measured spectrum by assuming that the optical constants of the film follow a mathematical model [205]. With this method, the refractive index and the thickness of the monolayers are determined. The used program, inspired in this method, was developed by the Optical Characterization Group of the Universitat de Barcelona [206].

Two mathematical models can be used for the fitting of the measured data. One of them is the Cauchy model, useful for dielectric materials, far from the absorption band [204]. Cauchy's equation is an empirical relationship between the refractive index n and wavelength of light λ for a particular transparent material. The most general form of Cauchy's equation is:

$$n(\lambda) = A + \frac{B}{\lambda^2} + \frac{C}{\lambda^4} \quad (5.6)$$

$$k(\lambda) = De^{\frac{E}{\lambda}}$$

where A , B , C , D , and E are coefficients (usually quoted for λ in micrometres) that can be determined for a material by fitting the equation to measured refractive indices at known wavelengths.

For porous silicon, the refractive index and the extinction coefficient can also be modelled with the Bruggemann Effective Medium Approximation (EMA), where it is assumed that the porous silicon layer is a mixture of the substrate silicon and air [207]. For this method, the dielectric constants of the components are named ε_i , f_i their volume fractions and y the screening parameter, the mathematical expression for the effective dielectric constant ε in terms of named ε_i , f_i and y is given (in implicit form) by

$$0 = \sum_i f_i \frac{\varepsilon_i - \varepsilon}{\varepsilon_i + y\varepsilon} \quad (5.7)$$

These methods enable the fitting of the reflectivity spectrum, obtained with the FTIR spectrometer; the fitting of the ellipsometric data, obtained with the ellipsometer, or the simultaneous fitting of both types of measured data.

The best fit can be obtained using simultaneously the reflectivity and the ellipsometric data. By this way, the optimal fit using measurements with two different techniques can be realized. In Fig. 5.18 and Fig. 5.19 the best fit obtained using both types of measured data can be observed for an example porous silicon layer. This monolayer was obtained by applying $J=20 \text{ mA/cm}^2$ for 120 s. For this case the Cauchy model was applied. The values obtained with this simultaneous fitting are a refractive index varying from 1.92 at $0.9 \mu\text{m}$ wavelength to 1.85 at $4 \mu\text{m}$ and a thickness of $2.43 \mu\text{m}$.

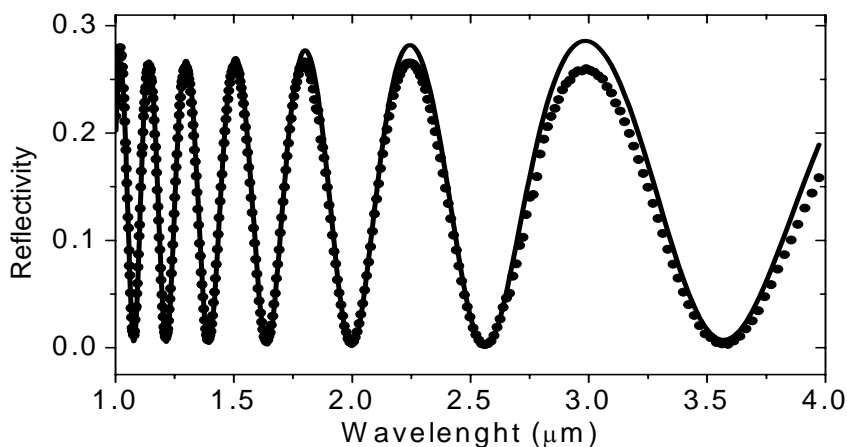


Fig. 5.18. Reflectivity spectrum of the porous silicon monolayer obtained with $J=20 \text{ mA/cm}^2$ and $t=120 \text{ s}$, measured with the FTIR spectrometer (symbols). The best least-squares fitted simulated spectrum is also shown (line).

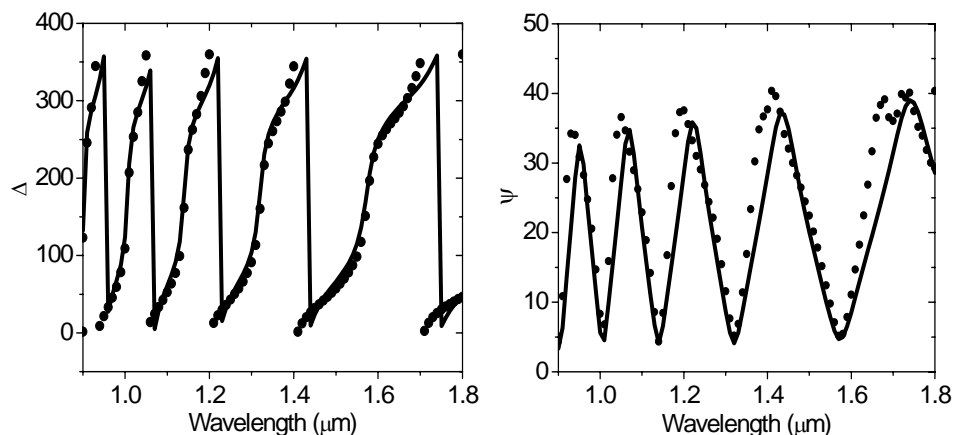


Fig. 5.19. Measured ellipsometric data Δ and Ψ (symbols) of the same porous silicon monolayer and the best least-squares fitted simulated ellipsometric data (line).

In Table 5.I we can compare the refractive indices obtained with the two explained methods, for this example porous silicon monolayer. The refractive index obtained with the Cauchy model agrees with the one calculated with the interference fringe method presented in the previous section. The thickness of the layer also agrees with the one determined with SEM. This agreement indicates that both methods are suitable for the calculation of the refractive index and thickness of porous silicon layers.

Method	Refractive index (for $\lambda=0.9 - 4 \mu\text{m}$)	Thickness (μm)
Interference fringes	1.97 - 1.83	2.48
Cauchy model	1.92 - 1.85	2.43

Table 5.I. Comparison of the refractive index and the thickness obtained with the method of the interference fringes and the Cauchy model. The porous silicon monolayer measured was obtained with $J=20 \text{ mA/cm}^2$ for 120 s.

5.3. Calibration of the fabrication system (Anodization parameters)

We have seen that the two most important characteristics of a porous silicon layer are its refractive index and its thickness. These two physical characteristics of the layers depend on two different parameters of the anodization process: the current density and the anodization time respectively. Therefore, it is essential to determine the relation between the physical characteristics of the layers and the anodization parameters.

The calibration of the fabrication system establishes the current density-refractive index relation and the etching time-thickness relation for each current density. These relations are basic for the fabrication of the porous silicon multilayer devices studied and designed in chapters 3 and 4.

For the calibration of the fabrication process, several monolayers fabricated with different current densities and etch times have been characterized using the methods described in the previous section.

5.3.1. Current density - Refractive index relation

The current density applied during the formation process determines the porosity of the porous silicon layer, and consequently its refractive index. The higher the current applied the higher the porosity and, therefore the higher the quantity of air in the layer resulting in a lower refractive index.

For each current density applied, a porous silicon layer with different refractive index is obtained. In Fig. 5.20 we can see the relation current density-refractive index established from the measurements of the fabricated porous silicon monolayers. These refractive indices have been calculated using the measurement of interference fringes method. In Fig. 5.20 we can observe that the decrease of refractive index is exponential with the current density. These results agree with the ones presented in the literature [208].

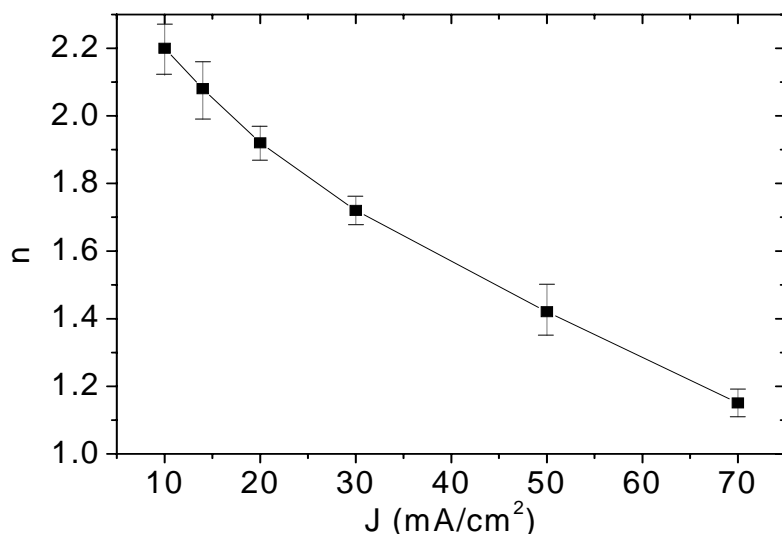


Fig. 5.20. Relation between current density and refractive index of porous silicon monolayers obtained with the bottom-wafer cell. The exponential dependence is also shown (black line). The bars indicate the variation of the refractive index for the wavelength range 1-4 μm .

The range of current densities studied goes from 10 to 70 mA/cm^2 . Current densities higher than 70 mA/cm^2 yielded very fragile porous layers where frequently the etched area was slightly detached from the substrate. Current densities lower than 10 mA/cm^2 yielded porous layers with very slow etch rates, increasing the duration of the layer formation without a significant gain in the index. Besides, these layers can be hardly seen with SEM, which highly hinders their characterization. These considerations have been taken into account for the design of the fabricated multilayer devices presented in chapter 7.

The current density-refractive index relation in Fig. 5.20 permits us to calibrate the porous silicon formation system because it establishes the relation between the electric parameters (J) and the physical characteristics of the porous silicon layer (n). To complete the calibration of the fabrication system,

the knowledge of the relation anodization time-thickness is essential. This relation is analyzed in the next section.

The porous silicon multilayer structures fabricated during the realization of this thesis are designed to work in the wavelength range from 1 μm to 4 μm . Hence, the calibration of the fabrication system has been analyzed for this wavelength range. The refractive index of porous silicon is not constant within this wavelength range. This variation can be observed in Fig. 5.21 where the refractive index of a porous silicon monolayer is represented. It can be observed that the refractive index is higher for 1 μm and decreases until approximately 1.5 μm . From this wavelength on, the decrease of the refractive index is very slow, quite constant. This variation has been represented in Fig. 5.20 using the variation bars for each point.

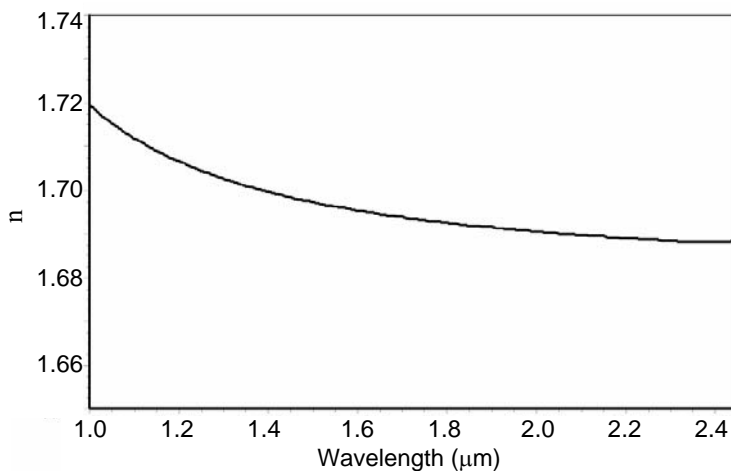


Fig. 5.21. Refractive index of a porous silicon layer simulated with a thin film EMA model for an example porosity of 35 %.

5.3.2. Current density - Porosity relation

One of the most important characteristics of a porous silicon layer is its porosity, defined as the fraction of air inside the porous layer. In fact, for the purpose of this thesis, the porosity of a layer is not an essential value but our essential parameter is the refractive index of the layer. As it has been explained before, for the simulation of any optical device the essential data of the layers that form the multilayer are the thickness and the refractive index, whereas the porosity is not used anywhere in the simulation and design process. Of course we know that the refractive index is determined by the porosity but for the simulation the concept porosity is completely invisible.

Similarly to simulation, for the fabrication the porosity is also “invisible” because the different methods used for the characterization of the porous silicon layers (interference fringes method and spectrum analysis fitting) calculate the refractive index and the thickness of the layers, not the porosity. However, here we present the relation between porosity and current density because it could be interesting for future applications of the porous silicon layers.

Fig. 5.22 the porosity-current density relation. These porosities have been calculated from the ellipsometric measurements (explained in chapter 7). In Fig. 5.22 we can observe that the porosity increases exponentially with the current density. The variation bars plotted for each current density are due to two different reasons. For $J < 20 \text{ mA/cm}^2$, we have concluded from the ellipsometric study that the porosity varies gradually in depth, being the porosity at the top of the monolayer higher than at the bottom of the monolayer. Therefore, the variation bars for these current densities indicate the top and the bottom porosity of the monolayer. For $J \geq 20 \text{ mA/cm}^2$, the pores of the porous silicon monolayers have not the same dimensions in all the directions, resulting in an anisotropic material. The variation bars for these current densities indicate these variations that are detailed explained in chapter 7.

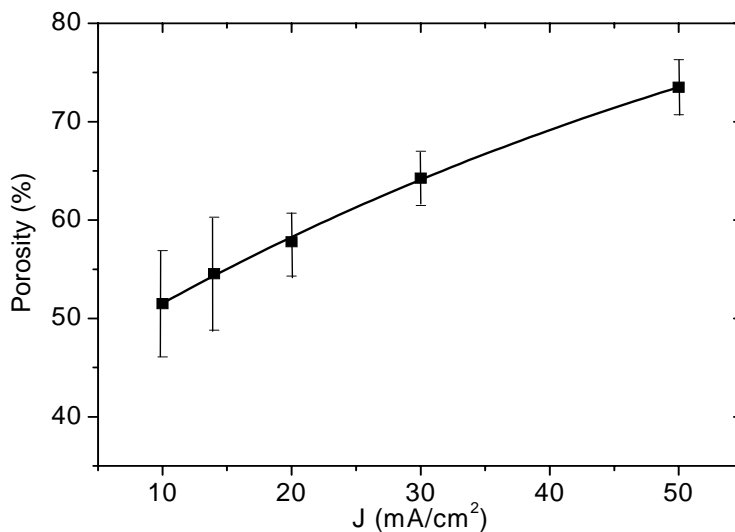


Fig. 5.22. Relation between porosity and current density. The exponential dependence is also shown (solid line).

5.3.3. Etching time - Thickness relation

The time during which a current density is applied is the etching time. It determines the thickness of the porous silicon layers. The anodization time-thickness relation for the fabricated porous silicon monolayers can be seen in Fig. 5.23, where the results for two different current densities are represented. It can be observed that it is a linear relation.

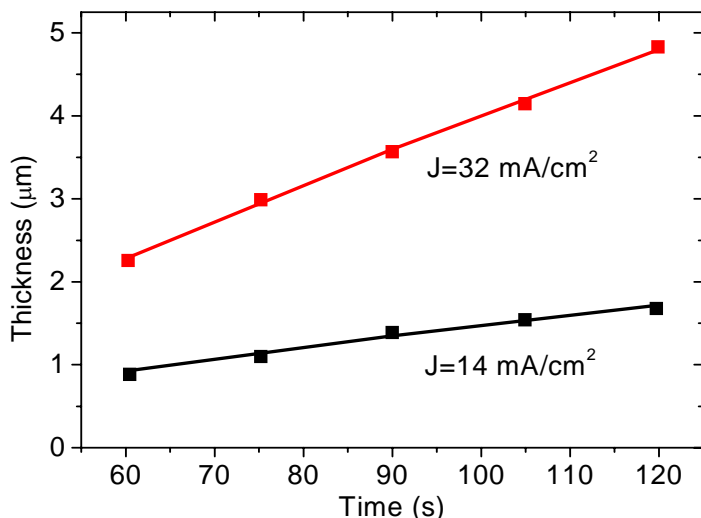


Fig. 5.23. Relation between the applied anodization time and the thickness of the monolayer, obtained for two different current densities (symbols). The lineal dependence is also shown (lines).

From this figure, we can also see that the slope is different for every current density and it increases when the current density increases. This slope let us define another formation parameter of porous silicon, the etch rate that is the velocity of formation of a layer with a certain porosity. In Fig. 5.24 the dependence of the etch rate with the current density is shown. From this figure we can conclude that the etch rate increases with the current density with exponential dependence. Another conclusion that we can obtain from Fig. 5.24 is that for high current densities, the fast etch rate hinders the fine control of the layer thickness. Also the precise control of the layer thickness is restricted by the "inertia" of the growth system.

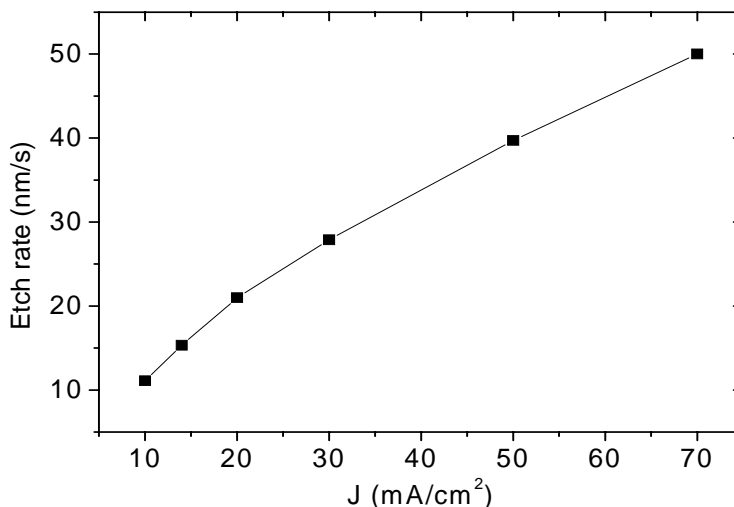


Fig. 5.24. Relation between de current density and the etch rate of porous silicon monolayers obtained with the bottom-wafer cell. The exponential dependence is also shown.

5.4. Conclusions

In this chapter we have explained two different processes: the fabrication and the characterization of the porous silicon layers.

The first part corresponds to the fabrication process and it explains in detail the porous silicon fabrication system established at the Department of Electronic, Electric and Automatic Engineering of the University Rovira i Virgili. The different elements that form this system have been presented and their influence on the porous silicon characteristics has been discussed. We have concluded that the structure of the electrochemical cell determines the homogeneity of the porous layers, being the most appropriate the cell where the silicon wafer is placed at the bottom and the electrolyte is stirred mechanically. The current source is another important element of the fabrication system because it determines the porosity and thickness of the porous silicon layers, and also the roughness of the interfaces. We have also concluded that the silicon wafers most suitable for the formation of microporous silicon are highly doped

p-type wafers (low resistivity). The rest of elements of the fabrication system are the electrolyte, being the one used an ethanol solution with 15 % HF concentration; and the control program realized for the control of the whole fabrication system, that has been also explained.

The characterization part is focused on the study of the fabricated porous silicon layers. The different measurement techniques used for the characterization of the fabricated porous silicon layers have been explained. These techniques are Scanning Electron Microscopy (SEM), Fourier Transform Infrared spectroscopy (FTIR) and Spectroscopic Ellipsometry (SE). From these measurements the two main characteristics of the porous silicon layers, refractive index and thickness, have been calculated using two different mathematical methods. The first is the interference fringes method that uses the SEM and the FTIR measurements to determine both refractive index and thickness. These two characteristics can also be calculated with the second method, the spectrum analysis fitting that uses the FTIR reflectivity spectrum and the ellipsometric measurements. The comparison of the results obtained with both methods indicates that both are equally suitable for the characterization of microporous silicon layers.

One of the applications of this characterization is the calibration of the fabrication system, that has permitted us to know well the system designed. This calibration has established the relations between the anodization parameters and the physical characteristics of the porous silicon layers, that are the current density-refractive index relation and the anodization time-thickness relation. The porosity has also been analyzed. We have concluded that the increase of the current density leads to an increase of the porosity and therefore a decrease of the refractive index. The relations of the current density with porosity and refractive index are both exponential. We have also concluded that the thickness increases linearly with the anodization time. From these values, we have also defined another parameter, the etch rate that is the velocity of formation of a porous silicon layer. The etch rate depends on the current density, basically it exponentially increases with current density.

Finally, the process for the fabrication of porous silicon multilayers has been explained. The values of the anodization parameters used for the formation of multilayers are based on the data given by the calibration process.